Mohan Saravanan[1]
Nurani Pabmanavhan Sambhamurthy[2]
Meenatchisundaram Sivarajan[3]

[1]Department of Biotechnology, Karpaga Vinayaga College of Engineering and Technology, Chinnakolambakkam, Maduranthagam, India
[2]Department of Chemical Engineering, Sathyabama University, Chennai, India
[3]Department of Chemical Engineering, Central Leather Research Institute, Chennai, India

Research Article

Treatment of Acid Blue 113 Dye Solution Using Iron Electrocoagulation

The electrocoagulation (EC) treatment of Acid Blue 113 (AB 113) was performed on the basis of chemical oxygen demand (COD) removal efficiency using an iron anode. The process variables, including current density (1–5 A/dm^2), pH (5.5–7.5), and supporting electrolyte concentration (1–3 g/L) were investigated. Under the optimum operating conditions, more than 91% COD removal efficiency was found. The optimum conditions were obtained with 3 A/dm^2 of current density, pH 6.5, and 2 g/L of supporting electrolyte concentration. COD removal rates obtained during the EC process can be described using a pseudo-kinetic model. The experimental kinetic data fit well with pseudo first-order kinetic model, with no significant change on the rate constant after 3 A/dm^2 of current density. The absorption spectra and Fourier transform infra red analysis were also performed to characterize the mechanism and nature of dye cleavage.

Keywords: Acid Blue 113; Chemical oxygen demand; Electrocoagulation; Fourier transform infra-red spectroscopy; Iron

Received: December 4, 2009; *revised:* March 19, 2010; *accepted:* March 21, 2010

DOI: 10.1002/clen.200900278

1 Introduction

The impact of pollution due to textile industry effluents has increased to significant extent. The dyes having an aromatic moieties linked together by azo (–N=N–) chromophore are the most important chemical class of synthetic dyes, representing about 60–80% of the organic dyes referenced in the color index (CI). These dyes have a variety of applications in the textile, paper, cosmetic, drug, and food industries [1]. The textile effluents, usually highly colored, could result in aesthetic problems when discharged as such into the environment. Conventional treatment of these wastewaters includes various combinations of biologic, chemical, and physical methods [2, 3]. These methods are becoming inadequate and insufficient due to large variability in the effluent composition.

One of the promising methods for treating wastewater streams is by electrochemical treatments. These processes (electrooxidation and electrocoagulation, EC) have been successfully employed for the removal of pollutants in various industrial wastewaters. The mechanism in the EC process includes coagulation, adsorption, precipitation, and flotation. Aluminum or iron electrodes are used in the process to produce their respective hydroxide flocks by oxidation reactions at anodes followed by hydrolysis. This EC technique is a very simple and efficient method for treating waste waters.

In recent years, EC has been applied successfully to treat water containing dyes, foodstuff wastes [4], oil wastes [4–6], suspended particles [7], organic matter from landfill leachates [7], chemical and mechanical polishing waste [8], synthetic detergent effluents [9], and mine wastes [10]. EC treatments for the textile dye-containing solutions or wastewater samples has been conducted on a laboratory scale; which showed good removal of chemical oxygen demand (COD), color, turbidity, and dissolved solids at various operating conditions [11–13]. This process is found to be very efficient in color removal with low-energy consumption.

In this study, Acid Blue 113 (AB 113, diazo) dye was taken, which is widely used in wool dyeing to obtain deep shade of navy blue color. These dyes have a high affinity for the fiber substrates and better fastness of color could be achieved. When effluents containing these dyes are released into the environment, it can cause long-term adverse effects on aquatic organisms. The objective of the study is to evaluate the treatment of CI AB 113 synthetic dye solution by EC process using an iron anode. In addition, the effects of pH, electrolyte concentration, and operational variables such as current density and treatment time are calculated based on the color and COD removal efficiency. The absorption spectra and Fourier transform infra red (FTIR) analysis are also carried out to evaluate the nature of bond cleavage.

1.1 Mechanism of Electrocoagulation

It is known fact that EC is a complex and interdependent process. The sacrificial anode produces coagulating agent to dose the dye solution while electrolytic gases are generated at the cathode [14]. The process of EC involves three successive steps:

1. Formation of coagulants by electrolytic oxidation of the ''sacrificial electrode,''
2. Destabilization of the contaminants, particulate suspension, and breaking of emulsions and,
3. Aggregation of the destabilized phases to form flocs.

Correspondence: M. Sivarajan, Department of Chemical Engineering, Central Leather Research Institute, Chennai 600020, India
E-mail: sivarajan_clri@yahoo.in

Abbreviations: **AB 113**, Acid Blue 113; **COD**, chemical oxygen demand; **EC**, electrocoagulation; **FTIR**, Fourier transform infra red.

In the present case EC has been performed using an iron electrode; the mechanism can be explained as follows [15]. Iron upon oxidation in an electrolytic system produces iron hydroxide, $Fe(OH)_n$, where, $n = 2$ or 3. The mechanism involved in the production of $Fe(OH)_2$ and $Fe(OH)_3$ are as follows:

Anode (Fe):

$$Fe_S \rightarrow Fe^{2+}_{(aq)} + 2\,e^- \qquad (1)$$

Cathode (Steel):

$$2\,H_2O_{(1)} + 2\,e^- \rightarrow H_{2(g)} + 2\,OH^-_{(aq)} \qquad (2)$$

The formation of insoluble $Fe(OH)_2$ with the release of OH^- ions at the cathode can be given by:

$$Fe^{2+} + 2\,OH^-_{(aq)} \rightarrow Fe(OH)_{2(S)} \qquad (3)$$

These insoluble $Fe(OH)_2$ precipitates at pH > 5.5 and remains in equilibrium with Fe^{2+} up to pH 9.5 or with monomeric species such as $Fe(OH)^+$, $Fe(OH)_2$, and $Fe(OH)_3$ at higher pH values [16]. The overall reactions (1)–(3) can be given by:

$$Fe + 2\,H_2O \rightarrow Fe(OH)_{2(S)} + H_{2(g)} \qquad (4)$$

In the presence of O_2, dissolved Fe^{2+} is oxidized to insoluble $Fe(OH)_3$ as:

$$4\,Fe^{2+} + 10\,H_2O + O_{2(g)} \rightarrow 4\,Fe(OH)_{(S)} + 8\,H^+ \qquad (5)$$

At the cathode (Steel), the protons can be directly reduced to H_2 gas:

$$8\,H^+ + 8\,e^- \rightarrow 4\,H_{2(g)} \qquad (6)$$

The corresponding overall reaction obtained by combining reactions (1), (5), and (6) is:

$$4\,Fe + 10\,H_2O + O_{2(g)} \rightarrow 4\,Fe(OH)_{3(s)} + 4\,H_{2(g)} \qquad (7)$$

The $Fe(OH)_3$ coagulates from pH > 1.0, i.e., it is present in much stronger acidic media than $Fe(OH)_2$. Then, this precipitate can be in equilibrium with soluble monomeric species like Fe^{3+}, $Fe(OH)^{2+}$, $Fe(OH)_2{}^+$, $Fe(OH)_3$, and $Fe(OH)_4{}^-$ as a function of the pH range, which transform finally into $Fe(OH)_3$ [17].

Once the insoluble flocs of $Fe(OH)_{3(s)}$ are formed, it remains in the aqueous stream as a gelatinous suspension, which can remove the dissolved dyes by complexation or by electrostatic attraction, followed by coagulation. In the surface complexation mode, the pollutant (dye) acts as a ligand to chemically bind hydrous iron:

$$Dye - H_{(aq)} + (OH)OFe_{(S)} \rightarrow Dye - OFe_{(S)} + H_2O_{(l)} \qquad (8)$$

The prehydrolysis of Fe^{3+} cations also leads to the formation of reactive clusters for water treatment [15]. The processes involved in an EC treatment: (i) the metal ions produced at the anode (Fe) and H_2 evolve at the cathode (steel) due to electrode reactions; (ii) formation of coagulants in the wastewater and in turn these coagulants involved in removal of dyes by sedimentation or by electro flotation with evolved H_2; and (iii) other electrochemical reactions involving reduction of organic impurities and metal ions at the cathode and coagulation of colloidal particles [18–21].

During the dye removal process, chlorine/hypochlorite (ClO^-) formed by anodic oxidation of chloride occurs, which destroy pollutants adsorbed on the anode surface [22]. A series of reactions involved in chlorine oxidation are shown in Eqs. (9)–(12). The direct oxidation of chloride ion at the anode to yield soluble chlorine:

$$2\,Cl^- \rightarrow Cl_{2(aq)} + 2\,e^- \qquad (9)$$

If the local concentration of dissolved chlorine exceeds its solubility, then supersaturation drives the formation of bubbles of chlorine gas. As electrogenerated chlorine diffuses away from the anode and rapidly hydrolyzed to hypochlorous acid and chloride ion:

$$Cl_{2(aq)} + H_2O \Leftrightarrow HClO + H^+ + Cl^- \qquad (10)$$

In the bulk solution this acid is in equilibrium with ClO^- ion as follows:

$$HClO \Leftrightarrow H^+ + ClO^- \qquad (11)$$

The predominant species is $Cl_{2(aq)}$ until pH near 3.0, HClO in the pH range 3–8 and ClO^- for pH > 8.0. The concentration of electrogenerated ClO^- can be limited by its anodic oxidation to chlorite ion. It is also possible the loss of ClO^- by reduction to chloride ion at the cathode:

$$OCl^- + H_2O + 2\,e^- \rightarrow Cl^- + 2\,OH^- \qquad (12)$$

Hypochlorite generated in Eq. (11) is a strong oxidant that can oxidize aqueous organic compounds. Chiang et al. [23] found that anode material, current density, and chloride concentration had similar effects on chloride/ClO^- production efficiency.

The kinetics of the overall EC process in COD removal is described by a pseudo-kinetics model in which the rate constant depends on the applied current density. This model provides preliminary data for evaluating the reaction rate constants [24]. The kinetic rate equation representing the COD removal rate from the aqueous solution is described by the following first-order reaction kinetics:

$$\ln\left(\frac{[COD]_t}{[COD]_i}\right) = -k_1 t \qquad (13)$$

where, $[COD]_i$ is the initial COD value (mg/L), $[COD]_t$ is the COD value at any time, t (mg/L). The slope of the plot of ln ($[COD]_t/[COD]_i$) versus time gives the value of the rate constant k_1 (1/min).

2 Materials and Methods

2.1 Reagent

Acid blue 113 is a secondary diazo dye having the molecular formula ($C_{32}H_{21}N_5Na_2O_6S_2$) and molecular weight of 681.65. AB 113 purchased from Aldrich, is a water soluble azo dye yielding a blue colloidal solution and its solubility is better in organic solvents such

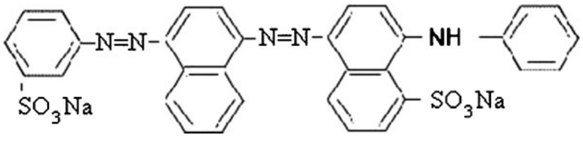

Figure 1. Schematic representation of the chemical structure of Acid Blue 113 dye.

as ethanol. All other reagents used in the experiment are of analytical grade. The structure of the dye is shown in Fig. 1.

2.2 Electrocoagulation Unit

The EC unit, given in Fig. 2 consists of a glass beaker of 250 mL capacity with a provision for fitting the electrodes. The electrodes used in the process are iron (grade MS 104) and stainless steel (grade SS 304) as anode and cathode, respectively, with a dimension of 4 cm × 4 cm. The spacing between the two electrodes is 2.5 cm. In each and every run, 200 mL of synthetic dye solution was treated containing an initial COD of 540 mg/L. The samples were collected at fixed time intervals and it was allowed to settle down for 20 min in the beaker before any analysis, as the degraded compounds settle down at this time noted. After the experiment, the power was switched off and the electrodes were disconnected. The experiments were carried out by connecting the electrodes to a DC regulated power supply (0–20 V, 0–5 A).

2.3 Experimental Procedure

The EC of AB 113 was investigated for different current densities (1–5 A/dm^2), pH (5.5–7.5), and electrolyte concentration (1–3 g/L). The samples were collected for every 10 min time interval and the absorbance was determined. The pH of the solutions was adjusted by adding 0.1 N sodium hydroxide (NaOH) or 0.1 N sulfuric acid (H_2SO_4) solutions. The pH of the aqueous sample was measured by means of a pH meter (1002). The dye concentration was determined using a UV–VIS spectrophotometer (Shimadzu, UV1020PC) at 580 nm. A standard solution of the AB 113 was scanned to determine the wavelength, λ_{max}, corresponding to maximum absorbance. The wavelength corresponding to maximum absorbance for AB 113 was found to be 580 nm. The concentration of AB 113 in the aqueous solution was estimated from the peak area of the absorption spectrum (200–800 nm) around λ_{max}, and by comparing the results to those of the known standard solutions.

The color removal efficiency was calculated by:

$$\text{Color removal efficiency}\,(\%) = \frac{(C_i - C_t)}{C_i} \times 100 \tag{14}$$

where, C_i is the initial concentration of the dye in solution (mg/L), C_t is the concentration of the dye at any time in solution (mg/L).

The COD removal efficiency was calculated by:

$$\text{COD removal efficiency}\,(\%) = \frac{([\text{COD}]_i - [\text{COD}]_t)}{[\text{COD}]_i} \times 100 \tag{15}$$

where, $[\text{COD}]_i$ is the initial COD value (mg/L), $[\text{COD}]_t$ is the COD value at any time, t (mg/L). The COD tests were performed, according to Standard Methods [25].

2.4 Absorption Spectra and FTIR Studies

The absorption spectra of the samples were recorded by scanning from 200 to 800 nm to check for the formation of intermediates and decolorization of the dye. The UV–VIS spectrum of AB 113 is observed and its change during EC was recorded using UV–VIS spectrophotometer. The characteristic peak of the pure dye was observed at 580 nm as already stated in the procedure. The pure dye compound and electro co-precipitated sludge generated during EC was analyzed using FTIR spectrometer. A 10–15 mg of sample was dispersed in 200 mg of spectroscopic grade KBr to record the spectra.

3 Results and Discussion

The effect of parameters such as current density, pH, and supporting electrolyte concentration on rate of COD removal was calculated. The rate of COD reduction has been plotted as COD/COD_i versus electrolysis time.

3.1 Effect of Current Density on the Efficiency of COD Removal

In electrochemical processes, the applied current density is an important factor that strongly influences the performance of EC [26]. The current density not only determines the coagulant dosage rate, but also the bubble production rate and size. Thus, this parameter should have a significant impact on pollutant removal efficiencies. A large current means a small EC unit. However, when

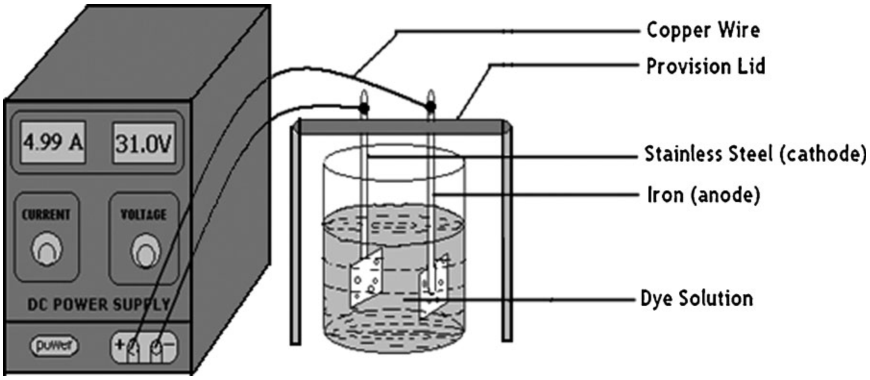

Figure 2. Experimental setup used for the electrocoagulation study.

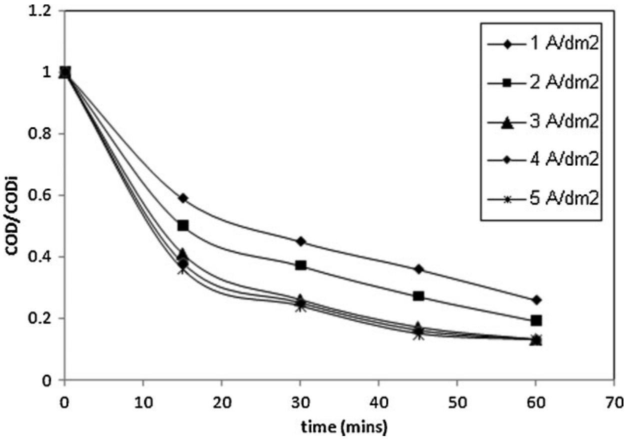

Figure 3. Effect of current density on COD removal. Conditions: initial COD 540 mg/L, supporting electrolyte concentration 2 g/L, and pH 6.5.

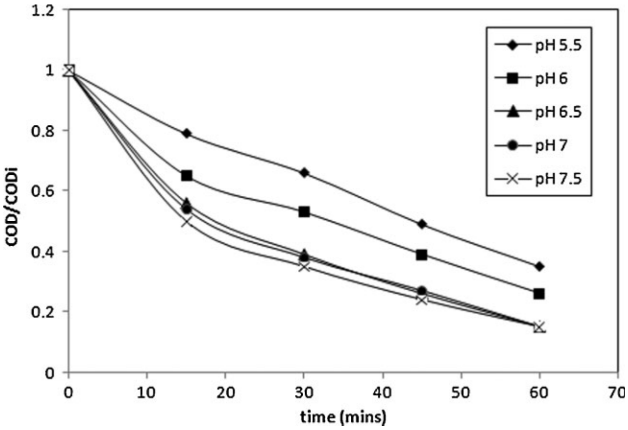

Figure 4. Effect of pH on COD removal. Conditions: current density 3 A/dm^2, initial COD 540 mg/L, and supporting electrolyte concentration 2 g/L.

too large amount of current is used, there is a high chance of wasting electrical energy in heating up water. To investigate the effect of current density on the AB 113 degradation rate, a serious of experiments were carried out with current density being varied from 1 to 5 A/dm^2, with initial concentration of 50 mg/L. The current density controls the generation rate of iron ions in the anode, the growth of $Fe(OH)_3$ flocs and the rate and size of H_2 bubbles evolved at the cathode [27].

The rate of degradation is high at the beginning of the process and decreases gradually at the end of the process. Figure 3 shows the rate of COD removal increases with increase in current density from 1 to 5 A/dm^2 may be explained that the rate of generation of ClO^- ion (Eq. (11)) increased with current density and thus increases the pollutant degradation, and after 3 A/dm^2 there is no significant COD removal. This can be ascribed to the fact that at high current, the amount of iron oxidized increased, resulting in a greater amount of precipitate for the removal of pollutants. In addition, the bubble density increases with increasing current density resulting in more efficient and faster removal. Moreover, the bubble size decreases with increasing current density, which is beneficial to the separation process and lowest current should be selected to obtain the best removal rate. Kashefialasl et al. [28] observed the dye Acid Yellow 36 degrades with 85 % color removal with current density of 12.8 j mA^{-1} cm^{-2} in 6 min.

3.2 Effect of pH on the Efficiency of COD Removal

The influence of electrolyte pH on dye degradation has been verified with experiments conducted under acid, alkaline, and neutral conditions. The current density was maintained at 3 A/dm^2. The rate of degradation is higher in the acidic pH, may be due to OH^- ion stability and there is no significant degradation after attaining a pH of 6.5 represented in Fig. 4. This is because, at pH of 6.5 a majority of iron complexes (coagulants) are formed and it can be taken as the optimum pH for carrying out the EC process. The dye taken for the experiment is good with acidic pH, though there is no greater difference in COD removal after attaining the acidic pH.

The iron anode generates a majority of $Fe(OH)_3$ flocs (Eq. (7)), to remove rapidly the dye molecules by complexation or electrostatic attraction, followed by coagulation. In contrast, at pH < 3 soluble Fe is the dominant species and $Fe(OH)_3$ flocs are quite poorly produced, whereas at pH > 9.0 a part of $Fe(OH)_3$ is solubilized as $Fe(OH)_4^-$ and lower amount of dye can only be separated [16]. It is already mentioned in the EC mechanism, at pH of 6.5 very slow oxidation of Fe^{2+} takes place results in $Fe(OH)_3$ flocs as a significant end product for dye adsorption. Similar conditions were observed with dye Acid Yellow 23 degraded at pH 6 with 98% color removal [29] and Acid Red 14 degraded at pH 6–9 with greater than 93% color removal [30]. Thus, pH of 6.5 is taken to be an optimum condition for further experiments.

3.3 Effect of Supporting Electrolyte Concentration on the Efficiency of COD Removal

The influence of electrolyte (NaCl) concentration on the dye degradation has been carried out at with three different concentrations of electrolyte (1–3 g/L) by having a pH of 6.5 and current density of 3 A/dm^2 obtained from pervious optimization experiments. The rate of dye degradation increases with increase in electrolyte concentration. The ClO^- ions that are formed (Eq. (11)) can oxidize the organic compounds in the solution under operating pH condition; it acts as a strong oxidizing agent. The formation of these chloride or ClO^- ions will depend on the electrolyte concentration and applied current density. Higher Cl^- content promotes faster destruction of dyes because of the formation of greater concentration of active chlorine species from reactions (9)–(11). The degradation rate are higher in acidic medium with $Cl_{2(aq)}$ and HClO as active species than in alkaline solutions where the less potent ClO^- acts as oxidant [16].

At lower chloride concentration, the dye degradation is less, compared to higher chloride concentration probably because there are not enough ions to conduct the current and very less formation of HClO for the oxidation of dye solution. The concentration of NaCl above 2 g/L has no significant influence on the rate of degradation depicted in Fig. 5. Thus it may be concluded that the increasing electric resistance of the solution affects negatively the efficiency of the process.

Based on the above obtained optimum conditions, a comparison is made between percentage of COD removal and percentage of color removal, as shown in Fig. 6, it can be seen that the rate of COD removal is lower than the rate of color removal, indicating that the azo bond cleavage is the first step of the process followed by the aromatic ring cleavage, which was found to be more than 95% color removal efficiency and 91% COD removal efficiency.

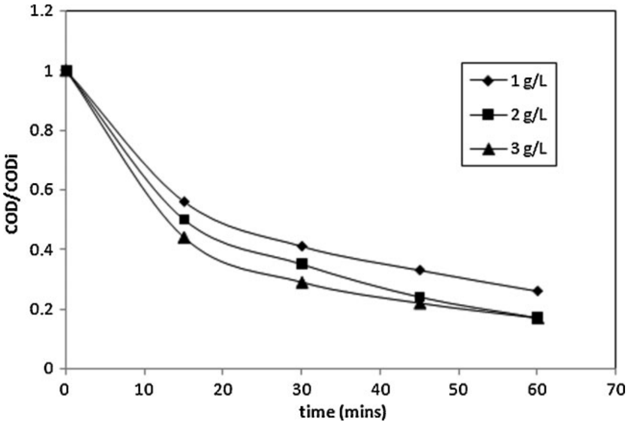

Figure 5. Effect of supporting electrolyte concentration on COD removal conditions: current density 3 A/dm^2, initial COD 540 mg/L, and pH 6.5.

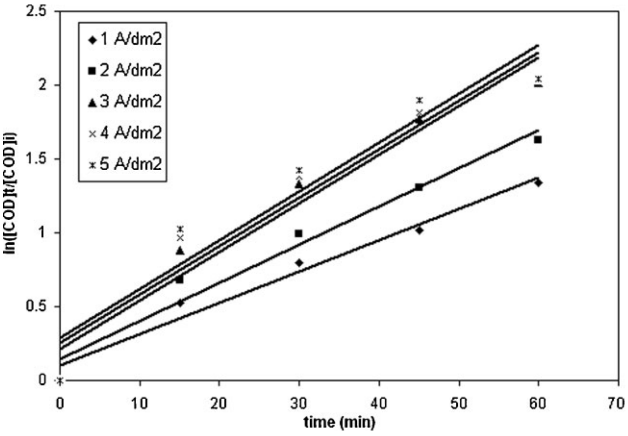

Figure 7. First-order reaction kinetics plot of iron electrocoagulation.

3.4 COD Removal Kinetics of Iron Electrocoagulation

It can be seen from the Fig. 3 that the COD removal efficiency increases with an increase in the applied current density. This can be explained that at high current densities, the extent of anodic dissolution of iron increases, resulting in a greater amount of precipitate for the removal of pollutants. In addition, the rate of bubble generation also increases with increasing current density, which enhances the COD removal efficiency. With this note, the kinetics of iron EC can be proposed from Eq. (13), where slope of the plot of $\ln (COD_t/COD_i)$ versus time gives the value of the rate constant k (1/min). Figure 7 shows the first-order reaction plot. The first-order kinetic model fits well with the observed data of the EC process. With other operating parameters kept constant, increasing applied current density from 1 to 3 A/dm^2 significantly enhanced the rate constant of COD removal. After 3 A/dm^2, there is no significant effect on the rate constant of COD removal shown in Fig. 8. The advantage of the present EC process takes very less time for greater COD removal, which can be noted.

3.5 Absorption Spectra Analysis

The mechanism of dye cleavage can be explored from the absorption spectra (UV–VIS spectra) of the dye solutions collected at 0 min (a) and 60 min (b) of the EC process, as shown in Fig. 9. It was observed that before treatment the dye was characterized by one main band in the visible region with a peak at 550 nm, and another band in the ultraviolet region with a peak at 290 nm and many uncharacterized peaks were found between 200 and 280 nm. The bands in the visible region from 450 nm to around 580 nm could be assigned to the n–π^* transition of —N=N— group and bands in the ultraviolet region around 290–300 nm could be attributed to the π–π^* transition related to the aromatic ring attached to the —N=N— group in the dye molecule.

It is apparent that the intensity of band at 550 nm was found to diminish rapidly with an increase in the time of EC process may be due to the electrophilic cleavage of azo bonds attached to the constituent benzene rings of the dye, while in the UV region the absorption gets increased, indicates the degraded intermediates were generated during the process. The disappearance of the bands in the visible region directly indicates the effective destruction of the chromophore. From the absorption spectra, it could be concluded that the dye molecule undergoes rapid cleavage to break the azo bonds in the presence of iron anode and this leads to a number of intermediates, which can be further studied by FTIR analysis.

3.6 FTIR Analysis

To understand the nature of adsorption of the dye and its degradation products, the various stages of degradation that occurs

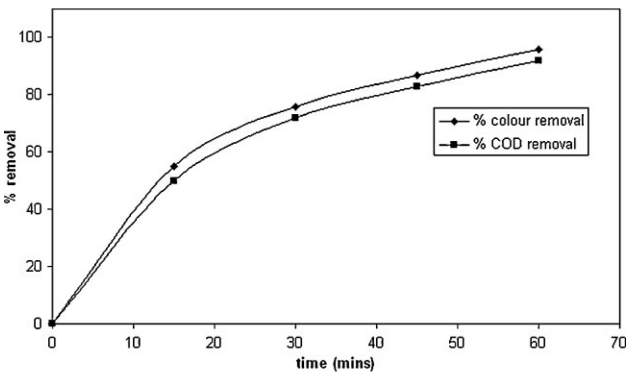

Figure 6. Comparison between percentage of COD and color removal.

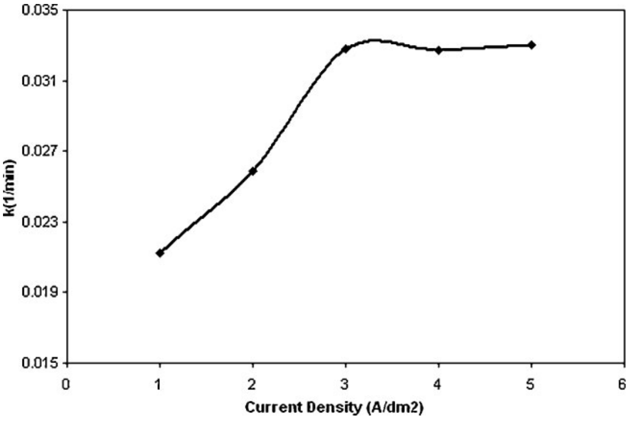

Figure 8. Effect of rate constant with increase in current density.

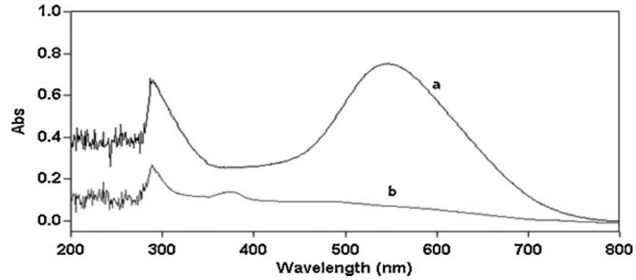

Figure 9. Absorption spectra a) initial dye solution, b) after 60 min of electrocoagulation.

during an EC process were analyzed by FTIR spectroscopic technique shown in Fig. 10. The FTIR spectrum of AB 113 (Fig. 10a) shows a broad and intense band at 3445 (1/cm). This could be attributed to stretching vibrations of OH groups. The sharp bands at 1596 (1/cm) and 1106 (1/cm) could be due to —N=N— and C—N stretching vibrations. The strong bands at 1384, 1348, 1305, 1032, 760, and 684 (1/cm) may be due to S—O stretching vibrations. The bands at 800 and 1305 (1/cm) could be assigned to C—O stretching vibrations. The bands at 1032, 800, 1106 (1/cm) corresponds to aromatic ring C—C stretching vibrations while the bands at 1596 and 1384, 1348 (1/cm) could be ascribed to C—H bending vibrations.

A strong and a broad band at 3400 (1/cm) and a low intensity peak at 1627 (1/cm) may be due to iron oxy-hydroxide (Fig. 10b) that attribute to stretching vibration of —OH and H—O—H bending modes of free water. The band at 1627 (1/cm) can be specifically ascribed to water adsorbed within the colloids of iron oxy-hydroxide. The weak transitions at 890 and 770 (1/cm) are probably due to Fe—O vibrations. The band at moderate intensity around 1023 (1/cm) and a low intensity band at 665 (1/cm) indicate the presence of α-FeOOH and Fe_2O_3, respectively. Thus the FTIR data suggests the formation of different iron oxides during EC.

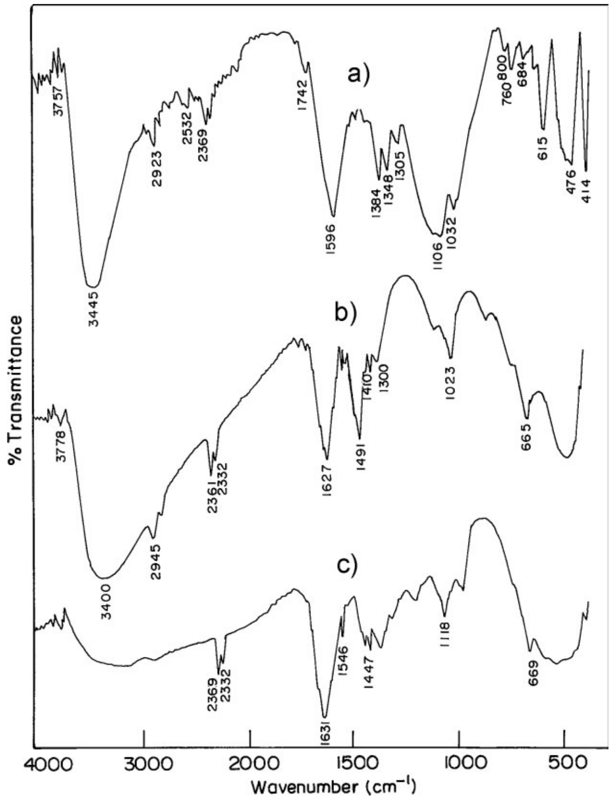

Figure 10. FTIR spectra a) Acid Blue 113 dye, b) iron oxy-hydroxide formation, c) after 60 min of electrocoagulation.

The FTIR spectrum at the end of the whole experiment is shown in Fig. 10c). The weak broadband up to 2369 (1/cm) confirms azo bond cleavage of the dye. It is interesting to note that the bands assigned to surface hydroxyls in the region of 3450–3650 (1/cm) are absent. The result shows that the degradation products is less toxic than that of the dye used and also conclude that the cleavage of azo linkage is adsorbed on iron oxy-hydroxide sludge formed during the EC process, which indicates the reduction in toxicity of the dye after degradation.

4 Conclusions

The present study demonstrated the removal of AB 113 dye solution by iron EC. It has been observed that the percentage of COD removal was significantly influenced by pH, current density, and supporting electrolyte concentration. Under optimum conditions, color removal (> 95%) and COD removal (> 91%) was found to be higher for the solution containing AB 113 dye. The experimental data fits well with first-order kinetics, showed no significant change in the rate constant after attaining the optimum current density (3 A/dm^2). The treatment of dye was also studied by absorption spectra showing no dye peak at the end of the process. FTIR analysis confirms the cleavage of azo bond present in the dye and the degraded products obtained after treatment was less toxic than the untreated dye solution. The results showed that iron EC was found to be a suitable method for maximum dye removal and in the treatment of the dye solution.

The authors have declared no conflict of interest.

References

[1] H. Zollinger, *Color Chemistry: Syntheses, Properties and Applications of Organic Dyes and Pigments*, VCH, Weinheim **1991**.

[2] S. H. Kang, C. H. Liao, M. C. Chen, Pre-oxidation and Coagulation of Textile Wastewater by the Fenton Process, *Chemosphere* **2002**, *46*, 923.

[3] Y. M. Slokar, A. M. L. Marechal, Methods of Decoloration of Textile Wastewaters, *Dye Pigm.* **1998**, *37*, 335.

[4] G. Chen, X. Chen, P. L. Yue, Electrocoagulation and Electroflotation of Restaurant Wastewater, *J. Environ. Eng.* **2000**, *126*, 858.

[5] N. Biswas, G. Lazarescu, Removal of Oil from Emulsions Using Electro-coagulation, *Int. J. Environ. Stud.* **1991**, *38*, 65.

[6] V. E. Cenkin, A. N. Belevstev, Electrochemical Treatment of Industrial Wastewater, *Effluent Water Treat. J.* **1985**, *25*, 243.

[7] N. S. Abuzaid, A. A. Bukhari, Z. M. Al-Hamouz, Ground Water Coagulation Using Soluble Stainless Steel Electrodes, *Adv. Environ. Res.* **2002**, *6*, 325.

[8] C. T. Tsai, S. T. Lin, Y. C. Shue, P. L. Su, Electrolysis of Soluble Organic Matter in Leachate from Landfills, *Water Res.* **1997**, *31*, 3073.

[9] B. M. Belongia, P. D. Haworth, J. C. Baygents, S. J. Raghavan, Treatment of Alumina and Silica Chemical Mechanical Polishing Waste by Electrodecantation and Electrocoagulation, *Electrochem. Soc.* **1999**, *146*, 4124.

[10] S. P. Novikova, T. L. Shkorbatova, E. Y. Sokol, Purification of Effluents from the Production of Synthetic Detergents by Electrocoagulation, *Soviet J. Water Chem. Technol.* **1982**, *4*, 82.

[11] D. R. Jenke, F. E. Diebold, Electroprecipitation Treatment of Acid Mine Wastewater, *Water Res.* **1984**, *18*, 855.

[12] S. H. Lin, C. F. Peng, Treatment of Textile Wastewater by Electrochemical Method, *Water Res.* **1994**, *28*, 277.

[13] A. Gurses, M. Yalcin, C. Dogan, Electrocoagulation of Some Reactive Dyes: A Statistical Investigation of Some Electrochemical Variables, *Waste Manage.* **2002**, *22*, 491.

[14] K. Chithra, R. Thilakavathi, A. A. Murugan, C. Marimuthu, N. Balasubramanian, Treatment of Textile Effluent Using Sacrificial Electrode, *Modern Appl. Sci.* **2008**, *2*, 38.

[15] M. Yousuf, A. Mollah, R. Schennach, J. R. Parga, D. L. Cocke, Electrocoagulation (EC) – Science and Applications, *J. Hazard. Mater.* **2001**, *84*, 29.

[16] A. C. Martínez-Huitle, E. Brillas, Decontamination of Wastewaters Containing Synthetic Organic Dyes by Electrochemical Methods: A General Review, *Appl. Catal. B Environ.* **2009**, *87*, 105.

[17] C. Barrera-Díaz, F. Ureña-Núñez, E. Campos, M. Palomar-Pardavé, M. Romero-Romo, A Combined Electrochemical-irradiation Treatment of Highly Colored and Polluted Industrial Wastewater, *Radiat. Phys. Chem.* **2003**, *67*, 657.

[18] J. G. Ibanez, M. M. Singh, Z. Szafran, R. M. Pike, Laboratory Experiments on Electrochemical Remediation of the Environment. Part 4. Color Removal of Simulated Wastewater by Electrocoagulation–Electroflotation, *J. Chem. Educ.* **1998**, *75*, 1040.

[19] O. T. Can, M. Bayramoglu, M. Kobya, Decolorization of Reactive Dye Solutions by Electrocoagulation Using Aluminum Electrodes, *Ind. Eng. Chem. Res.* **2003**, *42*, 3391.

[20] N. Modirshahla, M. A. Behnajady, S. Kooshaiian, Investigation of the Effect of Different Electrode Connections on the Removal Efficiency of Tartrazine from Aqueous Solutions by Electrocoagulation, *Dyes Pigm.* **2007**, *74*, 249.

[21] M. Y. A. Mollah, P. Morkovsky, J. A. G. Gomes, M. Kesmez, J. Parga, D. L. Cockec, Fundamentals, Present and Future Perspectives of Electrocoagulation, *J. Hazard. Mater.* **2004**, *114*, 199.

[22] X. M. Li, M. Wang, Z. K. Jiao, Z. Y. Chen, Study on Electrolytic Oxidation for Landfill Leachate Treatment, *China Water Wastewater* **2001**, *17*, 14.

[23] L. C. Chiang, J. E. Chang, T. C. Wen, Indirect Oxidation Effect in Electrochemical Oxidation Treatment of Landfill Leachate, *Water Res.* **1995**, *29*, 671.

[24] D. Lakshmanan, D. A. Clifford, G. Samanta, Ferrous and Ferric Ion Generation During Iron Electrocoagulation, *Environ. Sci. Technol.* **2009**, *43*, 3853.

[25] A. D. Eaton, L. Clesceri, A. Greenberg, *Standard Methods for the Examination of Water and Wastewater*, 19th edn, American Public Association, Washington **1995**.

[26] D. Pletcher, F. C. Walsh, *Industrial Electrochemistry*, 2nd edn, Chapman and Hall, London, UK **1990**.

[27] G. Chen, Electrochemical Technologies in Wastewater Treatment, *Sep. Purif. Technol.* **2004**, *38*, 11.

[28] M. Kashefialasl, M. Khosravi, R. Marandi, K. Seyyedi, Treatment of Dye Solution Containing Colored Index Acid Yellow 36 by Electro-coagulation Using Iron Electrodes, *Int. J. Environ. Sci. Technol.* **2006**, *2*, 365.

[29] N. Daneshvar, A. R. Khataee, A. R. Amani Ghadim, M. H. Rasoulifard, Decolorization of C.I. Acid Yellow 23 Solution by Electrocoagulation Process: Investigation of Operational Parameters and Evaluation of Specific Electrical Energy Consumption (SEEC), *J. Hazard. Mater.* **2007**, *148*, 566.

[30] N. Daneshvar, H. Ashassi-Sorkhabi, M. B. Kasiri, Decolorization of Dye Solution Containing Acid Red 14 by Electrocoagulation with a Comparative Investigation of Different Electrode Connections, *J. Hazard. Mater.* **2004**, *112*, 55.